Design and Implementation of an RFI Direction Finding System for SKA Applications

James Zekkai Middlemost Gowans

A dissertation submitted to the department of Electrical Engineering, University of Cape Town in fulfilment of the requirements for the degree of Masters of Science in Electrical Engineering

Supervisor:
Prof. M. Inggs

September 22, 2015

Contents

1 Introduction **7**
- 1.1 Background . . . 7
- 1.2 User Requirements . . . 7
- 1.3 Requirements Review . . . 9

2 Literature Review **10**
- 2.1 Stuff from Schleher . . . 10
- 2.2 Introduction . . . 11
- 2.3 Signals . . . 11
- 2.4 Overview of Direction Finding . . . 12
  - 2.4.1 Model . . . 12
- 2.5 Antenna Array Fundamentals . . . 12
  - 2.5.1 Array Manifold . . . 13
- 2.6 Geolocation . . . 14
- 2.7 Overview of Direction Finding . . . 14
- 2.8 Radiometer . . . 14
- 2.9 Direction Finding Techniques . . . 17
  - 2.9.1 Classes of Direction Finder Systems . . . 17
  - 2.9.2 Scanned beam . . . 17
  - 2.9.3 Crossed Loop . . . 18
  - 2.9.4 Adcock Array . . . 18
  - 2.9.5 Watson-Watt Evaluation . . . 19
  - 2.9.6 Doppler . . . 19
  - 2.9.7 Time Difference of Arrival . . . 21
  - 2.9.8 Amplitude Comparison . . . 22
  - 2.9.9 Phase Interferometry . . . 22
  - 2.9.10 Summary . . . 23

3 From Electronic warfare target location methods **24**
- 3.1 Model . . . 24
- 3.2 Amplitude Comparison Methods . . . 27
- 3.3 MSE Phase Interferometery . . . 27
- 3.4 Statistical Methods . . . 28
  - 3.4.1 Subspace Methods . . . 28
  - 3.4.2 Maximum Likelihood . . . 28

4 RF Chain **29**

5 Calibration **30**
- 5.1 iADC . . . 30

6 ROACH Firmware Design **32**
6.1 Software Setup . . . 32
6.2 ADCs . . . 32
6.3 Polyphase Filter Bank . . . 32
6.4 Cross Multiplier . . . 32
6.5 Vector Accumulator . . . 33

7 Software Interface **34**
7.1 Code Structure . . . 34
7.1.1 Control Register . . . 34

8 Field Trials **36**
8.1 Power supply . . . 36
8.2 Signal Source . . . 36

9 User Interface **38**

List of Figures

1.1 Meerkat dish 7

2.1 Using triangulation from multiple DF stations to ascertain the geographic location of a target. Source: [1] 16
2.2 Loop antenna and beam pattern 18
2.3 Crossed loop antenna and beam pattern 19
2.4 Left: model for adcock antenna showing N-S and E-W pairs. Right: Japanese implementation of array for 2 MHz direction finding. Src: [2] 20
2.5 Watson-Watt array processing technique using the Adcock array. Note that difference channels from crossed beams are formed 20
2.6 Model for Doppler DF system 22
2.7 Two-element phase interferometry. Note that as the element spacing (d) is more than half a wavelength there is ambiguity. 23

5.1 ADC input differential voltage vs output binary number. Src: iADC datasheet . 31

List of Tables

Nomenclature

RDF Radio Direction Finding

1 Introduction

1.1 Background

MeerKAT is a 64-dish radio telescope, aimed at being the precursor to the full Square Kilometer Array (SKA) radio telescope. There telescope require a RF-quite environment in order to be able to operate. The presence of Radio Frequency Interference (RFI) will at best interfere with the ability of the telescope to do science, and at worst destroy the sensitive receivers designed to cope with only very weak signals from space. It is for this reason that the array is being deployed in the Karoo desert, well away from built up areas and the RF signals that go along with built up areas. However, there is always the possibility that RFI will manifest. Although all equipment taken to site is tested for RFI before hand, if equipment malfunctions or is not configured correctly or shielded correctly, RFI may be introduces. As such, RFI management systems must be in place to aid in the detection and amelioration of RFI.

The purpose of this research is to design one of these systems: a device capable of detecting RFI sources and doing parameter estimation on them. The particular parameter of interest is the Angle of Arrival (AoA) . The process of ascertaining the AoA of RF is known as direction finding.

Figure 1.1: Meerkat dish

1.2 User Requirements

1. A system to perform direction finding of both impulsive and continuous wave (CW) RFI sources is to be designed.
2. They key deliverables of this project are a software package and a thesis report.
3. The software package should have the following functions:
   a) It should take in input from a correlator. This could either be time domain cross correlation for impulsive sources or frequency domain cross correlation for continuous sources.
   b) It should parse a configuration file which contains information about the array configuration and information about the output from the correlator.
   c) The data from the correlator should be used to ascertain the direction of the detected signals.

d) The software should be designed to fit into a system which has a 100% probability of intercept.

4. The software should have the following user interface features:
   a) The user should connect to it via a web interface.
   b) A streaming waterfall plot of frequency vs amplitude should be displayed to the user to serve as monitoring of the RFI environment.
   c) The user should be able to select a band of interest from the waterfall plot.
   d) The direction finding should then be computed for the signal in that band.
   e) The result of the DF should be presented to the user. An investigation must be done into the best way to present this information to the user.
   f) Where appropriate, additional meta information should be displayed to the user, such as measurement accuracy or signal strength.
5. The system should be designed to find terrestrial RFI sources.
6. The system should be designed to be location independent. It could either be deployed to a fixed location or as a mobile device deployed on a vehicle.
7. This project should be able to interface easily with other systems requiring its data. Specifically, it should be designed to interface with and pass its data on to an allied project which is doing classification of RFI.
8. The system should be real-time, where real-time is defined as having a latency in the order of a few seconds from receiving signals to displaying results to the user.
9. The hardware and software used should be in line with what is used at MeerKAT. This implies the ROACH platform for hardware, Python for back end software and JavaScript for front end software.
10. This system must operate in the context of the MeerKAT site, implying the following:
    a) In general, the RF environment is sparse. While there will be multiple simultaneous transmitters, it can be assumed there will only be one transmitter in a channel and one source of transients at a given time.
    b) The sources of the emissions will be relatively slow moving, up to the maximum speed of a vehicle on a dirt road; 60 km/h.
11. Once the software has been completed, its performance on real life data should be quantified in the following way:
    a) A prototype-stage 4-element antenna array should be connected to a 400 MHz baseband digitiser and correlator.
    b) The correlator need not be real time for the demonstration.
    c) As the goal of this project is not to develop a hardware system, there is no specific requirement on receiver sensitivity or noise figure. Whatever the best available hardware is should be used for the antennas, front end and digitiser.
    d) The performance of the hardware used should be analysed.

12. Mitigation of the effects of performance degradation due to multipath is outside of the scope of this work.

13. The report produced should contain a theoretical analysis of the performance of the system, as well as an analysis of the performance of the prototype on site with real signals.

1.3 Requirements Review

The requirements as stated by the SKA are understood and found to be acceptable.
(what else should go here?)

2 Literature Review

As discussed by (Electronic warfare and radar systems engineering handbook), in Electronic Warfare, AoA is the most critical parameter in hostile emitter sorting as it cannot be varied from pulse to pulse by the emitter. This may not directly translate to RFI hunting as emitters are not intentionally being hostile, but the RFI sources are still constrained in that their AoA parameter cannot be altered and hence is useful.

2.1 Stuff from Schleher

The simplest way to do DF is scan a narrow beam antenna. The position of the antenna which produces the highest output is the AoA. The antenna can be scanned physically by rotating it or electronically by a phased array. The down side of this approach is it cannot DF transients as it has a low POI. Well, POI as well as it needs time to scan around to figure out where the highest amplitude signal is.

Angular accuracy is:

$$\Delta\theta = k\theta_B/\sqrt{SNR} \tag{2.1.1}$$

Interferometer systems which use phase comparison for DF have a comparatively higher angular accuracy and rapid response which is good for transient detection. However, they impose stringent requirements on the phase matching for the RF chain which requires careful design, measurement and calibration.

Selection of antenna spacing necessitates a trade off between angular accuracy and ambiguity. The further the elements are placed apart, the greater the accuracy, but the more ambiguity is introduced. It is well known that for a 2-element array, the lowest ambiguity which can be achieved is 180° which is when the elements are spaced half a wavelength apart. Of course, this $\lambda/2$ is only valid for a single frequency. As soon as a different frequency needs to be received, the antennas will appear closer together or further apart, depending on whether the new frequency is higher or lower. As such, the specing is generally set by the highest frequency needed to be received, which puts an upper bound on the amount of ambiguity in the system.

For a linear array, the array is often constructed with a long baseline (in the order of 16λ) to provide high angular accuracy, and a short baseline $\lambda/2$ to resolve the ambiguity introduced by the system. It must be noted that with a linear array, there is always an unresolvable 180° ambiguity, no matter how many elements are present.

DF can also be done via Doppler shift which involves rapidly switching which antenna is sampled in an array to simulate rapidly rotating the antenna. When the antenna is being switched toward the signal source, the received frequency will go up. When the sampled antenna is being switched away from the source, the frequency will go down. By seeing at which stage of the switching the frequency is increasing and at which stage it is decreasing, it can be determined where the source is.

TODO: insert summary table from page 384 here.

Geolocation is done by measuring AoA from multiple locations and then triangulating to ascertain the true location of the source. This is outside the scope of this project. This project seeks only to design an AoA system. Not a geolocation system.

Probability of Intercept (POI) is a measure of the probability that the parameters of the EW receiving system match those of the target signal source at an instant in time. The key parameters are frequency and orientation. Frequency refers to whether the receiver is receiving on the frequency which is being transmitted. Orientation refers to whether the antennas of the receiver are pointed towards the signal source. For a 100 % POI, the receiver needs to be wide open (as opposed to narrow-band scanning) and have omni directional antenna coverage. This 100 % POI is essential to be able to intercept transient or impulsive signals.

2.2 Introduction

The purpose of this chapter is to provide a discussion into current strategies and implementations of direction finding systems. An analysis of the advantages and disadvantages of the various systems will take place which will aid in the later descision of which strategy to adopt for this project

2.3 Signals

As discussed by [3]:

We are interested in extracting the parameters of a signal. This is what sensor array signal processing does.

We model the E-field of a narrow-band signal by:

$$E(\vec{r},t) = s(t)\exp\left\{j(\omega t - \vec{r}^{\intercal}\vec{k})\right\} \tag{2.3.1}$$

Where:

- $s(t)$ is the slow (compared to the carrier) modulating signal with bandwidth B
- ω is the carrier frequency
- $\vec{r}$ is the radius vector, of form $\big[x, y, z,\big]$.
- $\vec{k} = \alpha\omega$ which is the wave-vector where $\alpha = \frac{1}{c}$ pointing in the direction of propagation. Note that the magnitude of the wave-vector is known as the wave-number: $|\vec{k}| = k = \frac{\omega}{c} = \frac{2\pi}{\lambda}$. This implies: $\vec{k} = k(\cos\theta \sin\theta)^{\intercal}$ where θ is the angle of the incident wave.

If we have a receiver with a radius vector $\vec{r_r} = \big[x_r, y_r\big]^{\intercal}$

Note that as per the narrowband assumption is is assumed that the array aperture be much less than the inverse relative bandwidth (f/B)

It is shown that the output of an L-element array a L-dimensional vector of the steering vector scalar multiplied by the incident signal, given by

$$\vec{x}(t) = \vec{a}(\theta).s(t) \tag{2.3.2}$$

Here, $\vec{a}(\theta) = \big[a_1(\theta), a_2(\theta), ..., a_L(\theta)\big]^{\intercal}$ which is the steering vector.

Furthermore, it is shown that the principle of superposition applies. If there are M incident signals they are simply summed together:

$$\vec{x}(t) = \sum_{m=1}^{M} \vec{a}(\theta_m)\vec{s_m}(t) \tag{2.3.3}$$

This can be re-written in a more compact form (now adding noise to the model):

$$\vec{x}(t) = \mathbf{A}(\vec{\theta})\vec{s}(t) + \vec{n}(t) \tag{2.3.4}$$

Where:

- we have re-written $\sum_{m=1}^{M} \vec{a}(\theta_m)$ as a matrix of steering vectors

$$\mathbf{A}(\vec{\theta}) = \left[\vec{a}(\theta_1), \vec{a}(\theta_2), ..., \vec{a}(\theta_M)\right] \tag{2.3.5}$$

- we have re-written $\sum_{m=1}^{M} s_m(t)$ as a vector:

$$\vec{s}(t) = \begin{bmatrix} s_t(t) \\ .. \\ s_M(t) \end{bmatrix} \tag{2.3.6}$$

2.4 Overview of Direction Finding

2.4.1 Model

The model which will be discussed here is that presented in [1].

Let there be N individual signal sources, where $\vec{s}(t)$ represents the resultant signal, being

$$\vec{s}(t) = \begin{bmatrix} s_1(t) & s_2(t) & s_3(t) & ... & s_N(t) \end{bmatrix} \tag{2.4.1}$$

Now let there be an array of M antenna elements receiving the signals, where the position of of the ith element is $\vec{x}_i = \begin{bmatrix} x_i & y_i & z_i \end{bmatrix}^\intercal$. The signal received by this ith element is influenced by the element position. This can be represented as $\vec{s}_i(t, \vec{x}_i)$, showing that the signal at an element is a function of the position of the element. As discussed by [3], as this model contains both spacial and temporal information, it is sufficient to be able to attain spacial information about the signal.

It is shown that the delay time for a signal arriving at the mth element is

$$\tau_m(\vec{\theta}) = \tau_m(\begin{bmatrix} \phi \\ \theta \end{bmatrix}) = \frac{1}{c}[x_m \cos(\phi)\cos(\theta) + y_m \sin(\phi)\cos(\theta) + z_m \sin(\theta)] \tag{2.4.2}$$

Where ϕ is the azimuth angle of the source and θ is the elevation angle. For a 2D space we let $\theta = 0$ and hence simplify to:

$$\tau_m(\phi) = \frac{1}{c}[x_m \cos(\phi) + y_m \sin(\phi)] \tag{2.4.3}$$

The $M \times 1$ steering matrix is

$$\vec{a}_k(\vec{\theta}_k) = \begin{bmatrix} e^{-j\omega_c \tau_1(\phi_k)} \\ e^{-j\omega_c \tau_2(\phi_k)} \\ ... \\ e^{-j\omega_c \tau_M(\phi_k)} \end{bmatrix} \tag{2.4.4}$$

2.5 Antenna Array Fundamentals

Here should be a discussion about how why arrays are necessary for DF. Then a discussion about some of the characteristics of an array.

2.5.1 Array Manifold

As discussed by [4] [5] [6].

The antenna array manifold is said to be useful for direction finding systems, as signal subspace techniques such as MuSIC rely on searching for the best $\vec{a}(p)$ for the detected signal [5].

It is shown by [6] that the output of an array of N sensors receiving M signals in the presence of noise is

$$\vec{x}(t) = \mathbf{A}(\vec{p})\vec{m}(t) + \vec{n}(t) \tag{2.5.1}$$

Where $\vec{x}(t)$ is the N-dimensional output of the array, $\vec{m}(t)$ is the M-dimensional set of signals received by the array, and $\mathbf{A}(\vec{p})$ is a $N \times M$ matrix of source position vectors (SPV). A given SPV, $\vec{a}(p_i)$, shows how the array responds to a source at location p_i, where p_i is often an azimuth and elevation pair: $p_i = (\theta_i, \phi_i)$.

For the case of a terrestrial-only system (which this project will be concerned with), ϕ can be set to 0, meaning that $p_i = \theta_i$, the azimuth angle of source i, typically in the range $[0, 2\pi]$. Here, a SPV can be simplified to $\vec{a}(\theta_i)$.

It is shown that if the N antennas are positioned symmetrically, the antenna array manifold is reduced from complex space $\mathbf{C}^N$ to real space $\mathbf{R}^N$ [6].

The response of the array to a source from a certain location, (θ, ϕ) is:

$$\vec{a}(\theta, \phi) = \vec{g}(\theta, \phi) \odot \exp\left\{-j\mathbf{X}^\intercal \vec{k}(\theta, \phi)\right\} \tag{2.5.2}$$

[6].

Where:

- $\vec{g}(\theta, \phi)$ is a N-dimensional vector of complex number being the gain and phase response of each element in the direction (θ, ϕ).
- $\mathbf{X}^\intercal$ is a $(N \times 3)$ matrix containing the x, y and z coordinates of each of the N elements of the form $\left[\vec{x}, \vec{y}, \vec{z}\right]^\intercal$
- $\vec{k}(\theta, \phi)$ is the wavenumber vector given by $\vec{k}(\theta, \phi) = \pi\left[\cos\theta\cos\phi, \sin\theta\cos\phi, \sin\phi\right]^\intercal$. Graphically, this equates to the

For the purposes of this research the elements will all be located at the same elevation as we only with to locate terrestrial signals. Hence, this may be simplified to:

$$\vec{a}(\theta) = \vec{g}(\theta) \odot \exp\left\{-j\mathbf{X}^\intercal \vec{k}(\theta)\right\} \tag{2.5.3}$$

Here, $\mathbf{X}^\intercal$ is now a $(N \times 2)$ matrix of the form $\left[\vec{x}, \vec{y}\right]$ and $\vec{k}(\theta) = \pi[\cos(\theta), \sin(\theta)]^\intercal$.

Furthermore, the $\vec{g}$ term may be excluded if we assume omnidirectional elements. Although it is rare to deal with true omnidirectional antennas, for an antenna which is required to receive signals only in the azimuth plane, omnidirectional antennas such as dipoles might very well be used in practice. This hence simplifies to:

$$\vec{a}(\theta) = \exp\left\{-j\mathbf{X}^\intercal \vec{k}(\theta)\right\} \tag{2.5.4}$$

Or, more expressively:

$$\vec{a}(\theta) = \exp\left\{-j\begin{bmatrix} x_1, y_1 \\ x_2, y_2 \\ .., .. \\ x_N, y_N \end{bmatrix}\begin{bmatrix}\cos(\theta) \\ \sin(\theta)\end{bmatrix}\right\} = \exp\left\{-j\begin{bmatrix} x_1\cos(\theta) + y_1\sin(\theta) \\ x_2\cos(\theta) + y_2\sin(\theta)) \\ .., .. \\ x_N\cos(\theta) + y_N\sin(\theta) \end{bmatrix}\right\} \tag{2.5.5}$$

Clearly, this is simply a vector of phase shifts introduced by each element in the array as a function of both the location of the element and the angle of the incident wave relative to some defined zero location and zero direction. It is said by [6] that this array manifold completely characterises the array. That paper goes into additional details on how the manifold may simplified for linear arrays, as well as the special properties which a manifold of a linear array possesses. This will not be discussed here as the array used for this DF system is not likely to be linear.

2.6 Geolocation

Geolocation refers to the process of finding the absolute position of a target, often in terms of a coordinate system like latitude/longitude/elevation. This information is often more useful than only knowing the direction which an emitter lies in. However, it is shown that by having multiple DF stations, the process of triangulation may be used to geolocate a device from direction bearings [1].

This process is shown graphically in Figure 2.1, where multiple DF stations (S_1 through to S_M) are used to locate the x,y,z coordinates of the target x_T. Note that this geolocation process in the figure is for airborne DF systems searching for a ground based target. However, the system could easily be simplified to a purely terrestrial process.

The relevance of this note about geolocation to this work is that it is not necessary to attempt to design a system which can do geolocation natively. Rather, a DF system can be design which can later be duplicated in order to provide geolocation capabilities.

2.7 Overview of Direction Finding

In this section, an analysis is made of different the direction finding techniques which exist. The most applicable of these will be examined in more details following. Classical methods of direction finding algorithms [7].

- Beamforming: by introducing the correct phase delay to each channel of the array, the array factor can be made to be such that the signal in quesetion is added coherently by each element of the array. This phase delay indicates the direction of arrival of the signal. The coherent addition of the signals allows for much higher SNR.

2.8 Radiometer

A radiometer is a device which is able to provide a very high accuracy approximation of noise power by averaging a large number of noise samples over a long time period. Due to the high accuracy measurements it can make, it is able to detect small changes in received power. It does this by achieving a high sensitivity. Sensitivity is the measure of how weak a signal and instrument is able to detect.

We will define power in terms of a matched load heated to a certain temperature observed over a certain bandwidth.

$$P = kTB \tag{2.8.1}$$

where $k \approxeq 1.38 \times 10^{-23}\,\mathrm{J\,K^{-1}}$, the Boltzmann constant.

System temperature is a combination of noise powers from atmospheric emissions, the warm earth, the cosmic microwave background, receiver noise figure, losses in the RF chain and others.

These noise sources mask the RFI signal which we are trying to locate. While typically an RFI signal below the noise floor would not be an issue, in the case of a radio astronomy reserver that signal will in all likelihood still be a problem because the noise floor of the MeerKAT array is so much lower than the RFI DF instrument. In essence, a signal which will be very loud to the telescope may be difficult for the DF system to even detect. Effort will hence need to go into ensuring that this instrument being designed will be able to see signals below its own noise floor.

As the noise at an antenna is a combination of a multitude of noise sources, the central limit theorem states that output of the antenna will be approximately a normal (Gaussian) distribution.

The noise temperature is defined as the noise power per unit bandwidth over the Boltzmann constant:

$$T_N = \frac{P_v}{k} \tag{2.8.2}$$

Assuming the power of a noise source remains constant, a single sample of the noise source has an RMS error of approximately $\sqrt{2}T_{sys}$. However, by integrating the noise power from a certain bandwidth ΔB over some integration time τ the error can be significantly reduced to

$$\sigma_T = \frac{\sqrt{2}T_{sys}}{\sqrt{2B\tau}} = \frac{T_{sys}}{\sqrt{B\tau}} \tag{2.8.3}$$

Where σ_T is the RMS error in the measurement of the noise temperature, T, and T_{sys} is the actual system noise temperature. Note that $2B\tau$ is the number of samples acquired

This process used in a radiometer of acertaining a high accuracy approximation of a received signal by integrating the signal over some observation period can also be used in the context of a direction finding system. For this application, a long observation period may be used to extract a weak signal which is burried in noise so that the weak signal may be processed.

$$\frac{S}{N} = \frac{S}{N}\sqrt{B\tau} \tag{2.8.4}$$

Tsys = Tsky + Trx where Tsky is thestuff above and Trx is Johnson noise from electronic components. Tsky can't do anything about. Trx lowered by cooling components. The Trx is as a result of the Johnson-Nyquist noise.

Extension to interferometry:

$SEFD/(N(N-1))/2\tau 2B)$

Sources: https://casper.berkeley.edu/astrobaki/index.php/Radiometer_Equation https://casper.berkeley.edu/astrobaki/index.php/Radiometer_Equation_Applied_to_Telescopes https://www.cv.nrao.edu/course/astr534/Radiometers.html

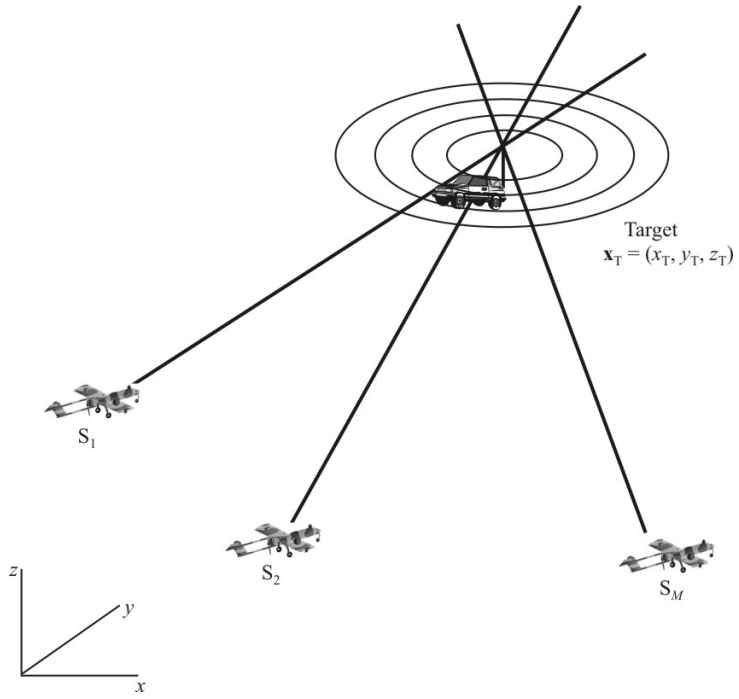

Figure 2.1: Using triangulation from multiple DF stations to ascertain the geographic location of a target. Source: [1]

2.9 Direction Finding Techniques

A Radio Direction Finder is a passive device able to ascertain the direction of a source of electromagnetic radiation which occurs in the RF frequency range, often defined as between 3 kHz and 300 GHz.

The general structure of a direction finding system is an antenna array connected to a receiver connected to a processing module connected to a display providing output to operators.

Radio DF has been around since the start of the 1900's. Some of the first people to work on DF systems were Marconi and Brown. One of the first systems developed by them was a device to locate the bearing from shore to a ship which was broadcasting a signal. Their device was used by manually rotated a two-element array with half-wavelength spacing to and monitoring the amplitude of the output of the antenna.

(Move this later): As discussed in [8], many high-performance DF algorithms which have been proposed over the years have had stringent requirements for array geometry or signal environment. The requirement for this project is for the system to be versatile and reconfigurable, so no such restrictions on array geometry or signal environment or modeling accuracy must exist.

2.9.1 Classes of Direction Finder Systems

The following overview of types of direction finding systems is based on discussions in the Electronic Warfare and Radar Systems Engineering Handbook [9]. In general, classes of system include:

2.9.2 Scanned beam

This is a direct amplitude technique. An antenna with gain (non-uniform beam) is rotated and this causes the power output of the antenna to vary with rotation angle. This is the earliest form of direction radio direction finding (RDF) and was implemented in the early 1900's. One of the first uses of this RDF device was to in a system developed by Marconi locate the bearing to a ship which was transmitting a signal for navigation purposes. A loop antenna was frequently used in the early 1900's as it was a simple antenna to construct and the beam pattern has a sharp null. An example antenna and beam pattern are shown in Figure 2.2. As the change in antenna output power per degree rotated is highest around the null, the antenna was often aligned such that the signal of interest was in the null. If multiple signals originating from different bearings are present, the system cannot operate. While today it may be possible to put highly selective receivers on the output of the antenna, this technology did not exist when scanning beam DF systems were originally used.

Note that as the beam pattern is symmetric about both the x and y axis, there are in general 4 ambiguous points. However, if the antenna can be rotated such that the signal is in the null, there is then only 2 ambiguous points, or 180° ambiguity. This can be resolved with an additional antenna element to resolve. Note also that this is not an instantaneous DF technique as it requires time for the antenna to be rotated. Hence, this technique is not suitable for finding transients.

Loop antennas DF systems are very sensitive to multipath errors, especially ionospheric reflection [10].

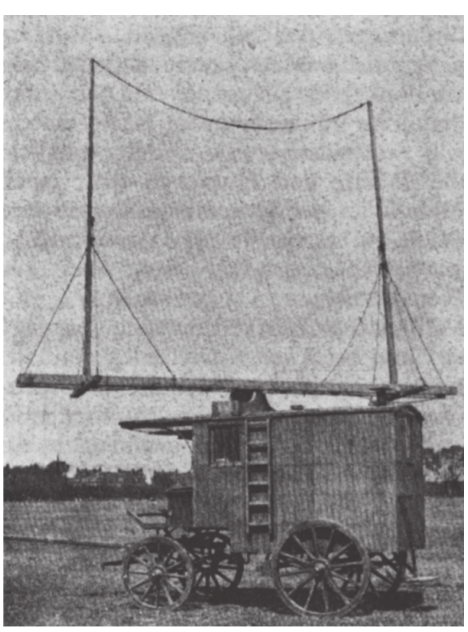

(a) Loop antenna used for direction finding in 1918. Src: [11]

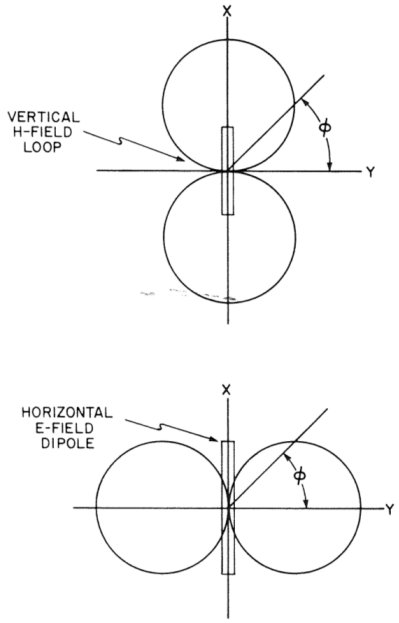

(b) Beam pattern of loop antenna or dipole. Note the sharp null. Src: [10]

Figure 2.2: Loop antenna and beam pattern

2.9.3 Crossed Loop

The crossed loop technique is an amplitude comparison technique. As is shown in Figure 2.3, using two loop antennas perpendicular to one another produces two beam patterns: one being proportional to the sine of the angle and the other to the cos of the angle. By comparing the signal power from each antenna, it is possible to ascertain the angle of arrival (AoA) . This system is instantaneous as only a single pulse is necessary to ascertain the ratio of antenna output power. However it has many ambiguities. Some ambiguities can be resolved with a sense antenna. For optimal ambiguity resolution, the crossed loop should be rotated such that signal of interest is located in the null of one of the loops and the peak of the other. This resolves ambiguity but at the expense of the system not being real-time. As with the scanned beam, the crossed loop suffers from significant performance degradation arising from multipath, specifically ionospheric reflection. In the 1930's a marine radio direction finder network using the crossed loop amplitude comparison technique was set up for marine navigation. Then, during World War II, rapid improvements to RDF technology were made with the operating frequency of the systems being extended into the VHF and UHF band and extensive RDF networks being installed [10].

2.9.4 Adcock Array

The Adcock array was developed and patented in 1919 by British army engineer Frank Adcock [12]. Instead of using loop antennas, the Adcock array makes use of two orthogonally orientated (crossed) pairs of monopole or dipole antennas. Typically a North-South pair and an East-West pair are used. These antenna pairs produce the same beam pattern as the loop antennas. As a loop antenna can be modeled by two vertical antennas on the sides and two horizontal antennas on the top and bottom of the loop, it should be clear that the loop is not polarisation selective.

(a) Example of crossed loop antenna.

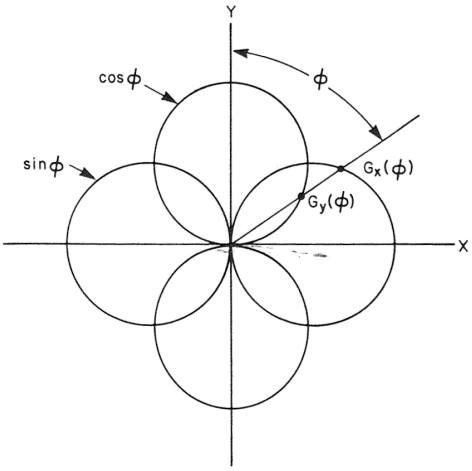

(b) Crossed loop antenna beam pattern showing difference in magnitude seen by each loop. Src: [10]

Figure 2.3: Crossed loop antenna and beam pattern

While the direct beam from the signal source may be vertically polarised, the reflected beam from atmospheric reflection was also being received and corrupting the signal output of the array. The Adcock array which uses only vertical elements maintains the same beam pattern as the loop but is not sensitive to horizontally polarised radiation hence offers better performance for a DF system. The antenna configuration of Adcock and Watson-Watt is shown in Figure 2.4. This array configuration was studied extensively in the 1930's and played a significant role in the electronic warefare of World War II [12].

2.9.5 Watson-Watt Evaluation

Ambiguity and multipath are one of the major difficulties which need to be overcome in direction finding systems. In the mid 1920s, Sir Robert Watson-Wat developed an improved DF system based on the Adcock array configuration. This is an amplitude comparison technique. As discussed above, the beam pattern of the output of an Adcock array is one cosine shaped beam and one sine shaped beam. By exploiting the trigonometric properties of these functions and adding an additional sense element, Watson-Watt developed a method to compute the angle of arrival from an array with this cos/sin property. This evaluation technique showed significant improvement in rejection of ionospheric reflections and made ambiguity resolution easier.

The mathematics around this technique will not be explored in detail here, but a graphical view of the antenna and receiver structure can be seen in Figure 2.5. For a more detailed discussion of the mathematics behind the Watson-Watt DF algorithm, see Poisel [13]. For a simulation of Watson-Watt algorithm as well as a discussion around an ambiguity resolution implementation using a sense antenna see: [14].

2.9.6 Doppler

By the principle of Doppler shift, moving an antenna towards a signal source increases the observed frequency while moving an antenna away from a source lowers the observed frequency.

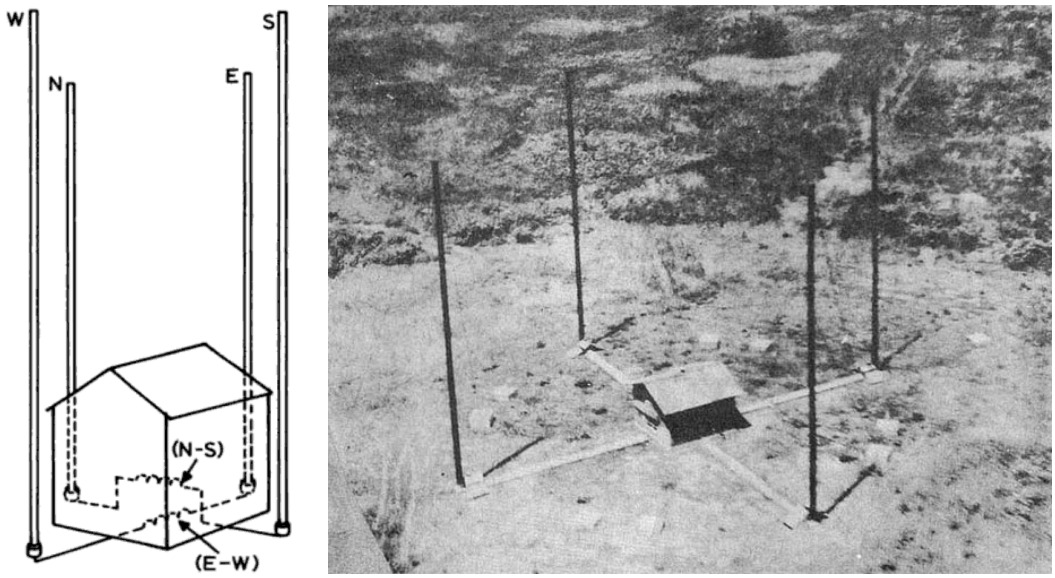

Figure 2.4: Left: model for adcock antenna showing N-S and E-W pairs. Right: Japanese implementation of array for 2 MHz direction finding. Src: [2]

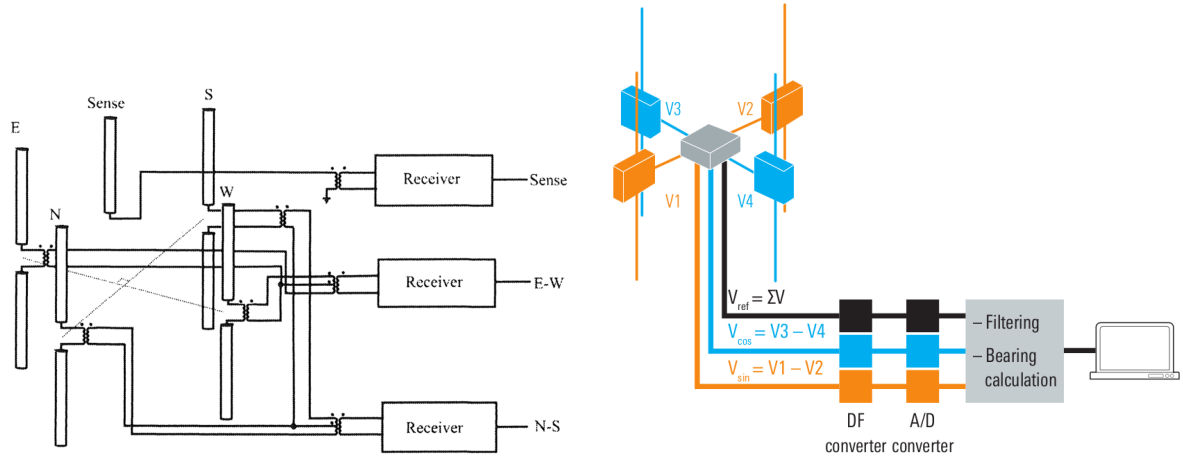

(a) View showing transformer configuration to produced required difference signals. Src: [13]

(b) Abstraced view of signal chain for digital processing. Src: [15]

Figure 2.5: Watson-Watt array processing technique using the Adcock array. Note that difference channels from crossed beams are formed

If an antenna is rotated around a central point (tracing out the circumference of a circle), there will be The Doppler shift is given by: [1]

$$\Delta f = \frac{B\omega}{c} f_c \sin(\Psi) \tag{2.9.1}$$

Where B is the length of the antenna baseline, ω is the angular velocity of the antenna, f_c is the carrier frequency of the signal source and Ψ is instantaneous difference between the angle towards the signal source and the angle of the rotating antenna (this is shown graphically in Figure 2.6. By rotating one antenna around a reference antenna and measuring the received signal frequency difference, the Doppler shift can be measured and with the above equation the AoA calculated.

However, As discussed by Jenkins, to DF a 100 MHz tone with a Doppler shift of 3 MHz, the antenna would need to be rotated with a tangential velocity of $10\,000\,\mathrm{m\,s^{-1}}$ [10]. It is not practical to rotate an antenna at such a high speed. Hence, rather than physically rotating an antenna, what is done in practice is that a Doppler shift is synthesised by rapidly switching between sampling different elements of a large circular array. Typically between 12 and 30 elements are used for Doppler DF arrays. Also graphically in Figure 2.6 is this typical implementation of a Doppler DF system using antenna switching.

As discussed by Jenkins [10], Doppler is not a high accuracy system due to the signal distortion introduced by switching the sampled antenna. Furthermore, Doppler DF is not suited to locating transients for two reasons:

1. it is not an instantaneous technique due to there being some time required to switch between sampling all of the antennas. For example, a typically time required to switch between all elements of an array may be 6 ms [15]. This is unsuitable for transients which may last only a few hundred nanoseconds.

2. it generally needs a narrow-band signal which has a well defined carrier frequency so that the Doppler shift is well defined. Impulsive transients do not have this characteristic.

For a more detailed discussion of the mathematics behind Doppler DF, see the Rhode & Schwarz report [15].

2.9.7 Time Difference of Arrival

TDOA is a DF system which is typically used for finding of impulsive sources; sources which emit a pulse that exists for a short time duration where the pulse has a clearly defined start and end. Most commonly it is used for locating pulsed radar system in the electronic warfare context.

For a two element array, the difference in time in the arrival of a pulse at the elements is

$$\delta t = \frac{d \cos\theta}{c} \tag{2.9.2}$$

Where d is the element spacing, θ is the AoA and c is the speed of light.

This technique requires the ability to measure the start of a pulse very accurately, or alternatively to be able to measure the difference very accurately through cross correlation.

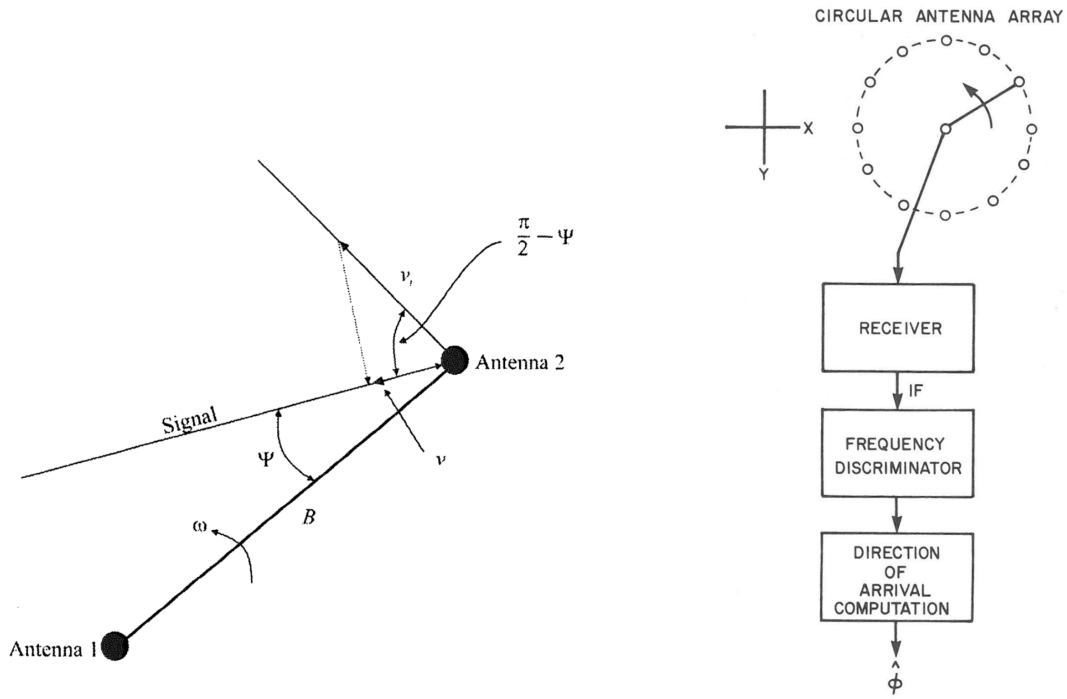

(a) Model for Antenna 2 rotating around stationary Antenna 1 with angular velocity ω. Src: [1]

(b) Practical implementation switching antennas for pseudo-Doppler DF system. Src: [10]

Figure 2.6: Model for Doppler DF system

2.9.8 Amplitude Comparison

This uses an antenna array. The antennas either have gain themselves or beam forming techniques are used to create beams with gains. Amplitude comparison techniques are in general simple to implement, but provide low resolution and low accuracy compared to phase methods due to their dependence on antenna beam pattern and their sensitivity to multipath. In practice, typical amplitude comparison systems have a DF RMS accuracy between 3° and 10°.

2.9.9 Phase Interferometry

This technique is done by comparing the phase arriving at each element of an array. In general, it is a high complexity technique and may suffer from ambiguity, but it can achieve comparatively high accuracy direction measurements, often between 0.1° and 3° for real systems. In comparison to amplitude systems, phase systems are more tolerant of multipath signals. The high complexity is introduced from having to carefully match the phases of the RF chains from each array element, and having to incorporate ambiguity resolution algorithms. Also, doing real-time high accuracy phase measurements of the signals at multiple antennas is often computationally complex.

The simples phase interferometry system is a two element array. This is shown graphically in Figure 2.7 where d is the element spacing, λ is the wavelength and θ is the AoA or difference between the boresight and wavevector. The phase difference at the output of the system is calculated as follows:

$$\phi = \frac{2\pi d \sin\theta}{\lambda} \tag{2.9.3}$$

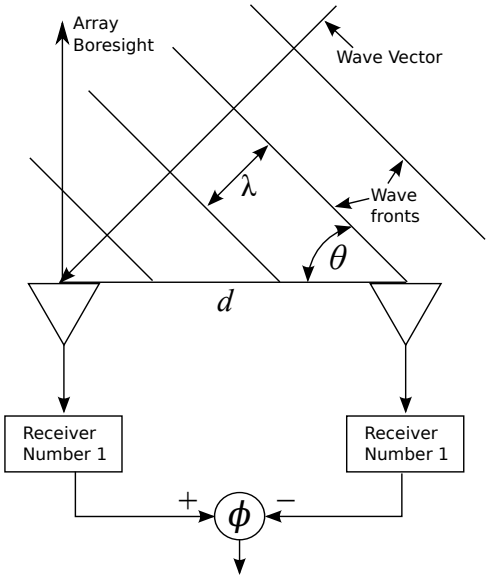

Figure 2.7: Two-element phase interferometry. Note that as the element spacing (d) is more than half a wavelength there is ambiguity.

Notes about this simple two element array:

1. The values of the sine function of only unique between $-90°$ and $90°$. Hence, the output of the array is only unambiguous over this $180°$ field of view. A two element phased interferometry array cannot resolve this ambiguity. The best it can do is use antennas with gain to reject signals from outside of its field of view.

2. If the element spacing is larger than $\frac{\lambda}{2}$ (as shown in the figure) the ambiguity gets worse. The unambiguous field of view for a 2-element array is: $\theta_{FOV} = 2\sin^{-1}(\frac{\pi}{2d})$. Clearly, as d gets larger θ_{FOV} gets smaller.

3. Although ambiguity gets worse with a larger spacing, angular accuracy improves. This is because the system has a percentage RMS error and when the FOV is shrunk, the error in degrees (which is a percentage of the FOV) also decreases. Hence, there is a trade-off between ambiguity and accuracy. This is an important note!

The solution to this ambiguity problem is to use more than two elements, thereby constructing a multiple baseline interferometer.

2.9.10 Summary

Amplitude based systems generally used for DF of cooperative emitters [10]

3 From Electronic warfare target location methods

This content comes from [1]. It should not be a chapter but rather be merged into the lit review.

Objective to find location of non-cooperative targets. Relevant to warfare as well as RFI.

Position fix can be ascertained by intersecting multiple lines of bearing (LOB). Or: AoA can be used in PF algorithms. Limiting factors to LOB: noise, measurement errors, multipath reflections.

Maximum likelihood estimation: original technique used for LOB to PF. Least-square error: other technique. Total LSE: more general.

Systematic errors: bias. Random errors: noise.

LSE: Find a solution to an overestimated system: more measurements than unknowns. Relies on minimising the cost function: sum of the square of the errors (difference between estimate and measurement). I could write some pretty maths here, but I actually don't understand it.

LSE is the same as maximum likelihood when noise is normally distributed.

3.1 Model

The model which will be discussed here is that presented in [1].

Let there be an array of M antenna elements receiving signals, where the position of of the mth element is $\vec{x}_m = \begin{bmatrix} x_m & y_m & z_m \end{bmatrix}$. The signal received by this mth element is influenced by the element position. This can be represented as $\vec{r}_m(t, \vec{x}_m)$, showing that the signal at the mth element is a function of the position of the element. As discussed by [3], this model contains both spacial and temporal information and hence is sufficient to be able to attain spacial information about the signal.

It is further shown by Poisel that the delay time for a signal arriving at the mth sensor from a source located at azimuth angle θ and elevation angle ϕ is

$$\tau_m(\vec{\theta}) = \tau_m(\begin{bmatrix} \theta \\ \phi \end{bmatrix}) \tag{3.1.1}$$

$$= \frac{1}{c}[x_m \cos(\theta)\cos(\phi) + y_m \sin(\theta)\cos(\phi) + z_m \sin(\phi)] \tag{3.1.2}$$

This model assumes that the azimuth and elevation angle to the source, $\begin{bmatrix} \theta & \phi \end{bmatrix}^\intercal$, is the same for each sensor. This is approximately true when the distance from the array to the source is much greater than the array geometry. Hence, it's often convenient and most accurate to select the center of the array as the origin. For a 2D space we let $\phi = 0$ and hence simplify to:

$$\tau_m(\theta) = \frac{1}{c}[x_m \cos(\theta) + y_m \sin(\theta)] \tag{3.1.3}$$

Expressed as a matrix multiply:

$$\tau_m(\theta) = \frac{1}{c}\begin{bmatrix} x_m & y_m \end{bmatrix}\begin{bmatrix}\cos\theta \\ \sin\theta\end{bmatrix} \tag{3.1.4}$$

$$= \frac{1}{c}\vec{x}_m\vec{k}(\theta) \tag{3.1.5}$$

Where $\vec{k}(\theta) = \begin{bmatrix}\cos\theta & \sin\theta\end{bmatrix}^\mathsf{T}$ is the wavenumber vector which graphically equates to the 'ratio' of how much the signal propagates in the x direction per distance propagated in the y direction. It's not really a ratio, it's a vector, so this doesn't quite makes sense. Note to self: tidy this up.

If this time delay is multiplied by the frequency in radians per second, ω, the result is the phase difference at the element relative to the origin:

$$\phi_m(\theta,\omega) = \omega\tau_m(\theta) \tag{3.1.6}$$

$$= \frac{\omega\vec{x}_m\vec{k}(\theta)}{c} \tag{3.1.7}$$

$$= \frac{\vec{x}_m\vec{k}(\theta)}{\lambda} \tag{3.1.8}$$

Representing the phase shift of all M sensors as a vector,

$$\vec{\phi}(\theta,\omega) = \frac{\mathbf{X}\vec{k}(\theta)}{\lambda} \tag{3.1.9}$$

Where $\mathbf{X}$ is a $(M \times 2)$ matrix containing the x and y coordinates of each of the M sensors. In general, the output of an array is also impacted by the amplitude scaling and phase shifting applied to the received signals by the beam pattern of each sensor. The combination of the phase shift resulting from the physical separation of the sensors and the amplitude/phase response of a sensor is a very key property of an array known as the antenna array manifold, or steering vector, or source-position vector:

$$\boxed{\vec{a}(\theta,\omega) = \vec{g}(\theta,\omega) \odot \exp\left\{j\frac{\omega\mathbf{X}\vec{k}(\theta)}{c}\right\}} \tag{3.1.10}$$

Often (as is the case in this project) the sensors used will be identical omnidirectional antennas. In this case, the amplitude and phase shift of the antennas as a result can be ignored, as it will be equal between elements and independent of angle or arrival.

$$\vec{a}(\theta,\omega) = \exp\left\{j\frac{\omega\mathbf{X}\vec{k}(\theta)}{c}\right\} \tag{3.1.11}$$

Or, more verbose:

$$\vec{a}(\theta,\omega) = \exp\left\{\frac{j\omega}{c}\begin{bmatrix} x_1, y_1 \\ x_2, y_2 \\ .., .. \\ x_M, y_M\end{bmatrix}\begin{bmatrix}\cos(\theta) \\ \sin(\theta)\end{bmatrix}\right\} \tag{3.1.12}$$

$$= \exp\left\{\frac{j\omega}{c}\begin{bmatrix} x_1\cos(\theta) + y_1\sin(\theta) \\ x_2\cos(\theta) + y_2\sin(\theta)) \\ .., .. \\ x_M\cos(\theta) + y_M\sin(\theta)\end{bmatrix}\right\} \tag{3.1.13}$$

$$\tag{3.1.14}$$

The vector output of the array, $\vec{r}(t)$, where each element of the vector is the signal received by the sensor is the where each element of the vector corresponds to an antenna element is equal to the sum of the signals at that element by the principle of superposition. Algebraically:

$$\vec{r}(t) = \sum_{k=1}^{K} s_k(t)\vec{a}_k(\vec{\theta}_k) + \vec{n}(t) \tag{3.1.15}$$

Where:

- $s_k(t)$ is the source signal,
- $\vec{\theta}_k = \left[\phi_k, \theta_k\right]^\intercal$ is the source parameter vector, a vector with azimuth and elevation angles pointing in the direction of the source,
- $\vec{a}_k(\vec{\theta}_k)$ is the antenna array manifold, explored more shortly,
- $\vec{n}(t)$ is additive noise.

Or in matrix notation:

$$\vec{r}(t) = \mathbf{A}(\vec{\theta})\vec{s}(t) + \vec{n}(t) \tag{3.1.16}$$

The array manifold vector is also known as source position vector or as the steering vector. It is the response of the array to a signal impinging on the array from a certain azimuth and elevation angle, (ϕ, θ). The response is naturally in terms of the gain and phase shifts introduced by each sensor as a result of the beam pattern and physical separation of the sensors. It is given by: [6].

$$\vec{a}(\theta, \phi) = \vec{g}(\theta, \phi) \odot \exp\left\{-j\mathbf{X}^\intercal \vec{k}(\theta, \phi)\right\} \tag{3.1.17}$$

Where:

- $\vec{g}(\theta, \phi)$ is a N-dimensional vector of complex number being the gain and phase response of each element in the direction (θ, ϕ).
- $\mathbf{X}^\intercal$ is a $(N \times 3)$ matrix containing the x, y and z coordinates of each of the N elements of the form $\left[\vec{x}, \vec{y}, \vec{z}\right]^\intercal$
- $\vec{k}(\theta, \phi)$ is the wavenumber vector given by $\vec{k}(\theta, \phi) = \pi\left[\cos\theta\cos\phi, \sin\theta\cos\phi, \sin\phi\right]^\intercal$. Graphically, this equates to the

For the purposes of this research the elements will all be located at the same elevation as we only with to locate terrestrial signals. Hence, this may be simplified to:

$$\vec{a}(\theta) = \vec{g}(\theta) \odot \exp\left\{-j\mathbf{X}^\intercal \vec{k}(\theta)\right\} \tag{3.1.18}$$

Here, $\mathbf{X}^\intercal$ is now a $(N \times 2)$ matrix of the form $\left[\vec{x}, \vec{y}\right]$ and $\vec{k}(\theta) = \pi[\cos(\theta), \sin(\theta)]^\intercal$.

Furthermore, the $\vec{g}$ term may be excluded if we assume omnidirectional elements. Although it is rare to deal with true omnidirectional antennas, for an antenna which is required to receive signals only in the azimuth plane, omnidirectional antennas such as dipoles might very well be used in practice. This hence simplifies to:

$$\vec{a}(\theta) = \exp\left\{-j\mathbf{X}^\intercal \vec{k}(\theta)\right\} \tag{3.1.19}$$

The antenna array manifold can now be re-written:

$$\vec{a}(\theta) = \exp\left\{-j\begin{bmatrix}\omega_c\tau_1(\phi_k)\\ \omega_c\tau_2(\phi_k)\\ \omega_c\tau_M(\phi_k)\end{bmatrix}\right\} \tag{3.1.20}$$

$$= \begin{bmatrix}e^{-j\omega_c\tau_1(\phi_k)}\\ e^{-j\omega_c\tau_2(\phi_k)}\\ ...\\ e^{-j\omega_c\tau_M(\phi_k)}\end{bmatrix} \tag{3.1.21}$$

Clearly, this is simply a vector of phase shifts introduced by each element in the array as a function of both the location of the element and the angle of the incident wave relative to some defined zero location and zero direction. It is said by [6] that this array manifold completely characterises the array. That paper goes into additional details on how the manifold may simplified for linear arrays, as well as the special properties which a manifold of a linear array possesses. This will not be discussed here as the array used for this DF system is not likely to be linear.

Let there be K individual signal sources, where $\vec{s}(t)$ represents the resultant signal, being

$$\vec{s}(t) = \begin{bmatrix}s_1(t) & s_2(t) & s_3(t) & ... & s_K(t)\end{bmatrix} \tag{3.1.22}$$

This important result shows us that for a known array with omnidirectional antennas at arbitrary x) and y locations, receiving a narrow band signal of known frequency from a certain direction, θ, the phase shift at each element is a vector which can be easily calculated. This is the basis around which the direction finding algorithm for this project will be designed.

3.2 Amplitude Comparison Methods

These methods, specifically the Wattson-Watt technique are probably the most commonly used DF methods over the history of DF systems [1]. They involve comparing the amplitudes of antenna beams. These beams can either be actual beams resulting from using antennas with gain, or as in the case of Wattson-Watt the beams can be synthesised by forming sum and difference channels from broad beam antennas in an array.

3.3 MSE Phase Interferometery

3.4 Statistical Methods

As per discussion in Poisel [1].

Statistical methods generally involve taking snapshots of the signals received at each sensor, $\vec{r}(t)$ and then calculating the covariance matrix of the received data. It can be shown that the covariance matrix is diagonal for incoherent sources, non-diagonal and non-singular[1] for partially coherent sources and non-diagonal and singular if at least one of the sources are coherent [1].

The direction finding process involves doing eigen analysis (finding eigenvalues and eigenvectors) for the covariance matricies. Two sorts of eigenvectors will be produced:

Noise Eigenvectors have an eigenvalue equal to the noise power.

Signal Eigenvectors have some property that I don't understand

3.4.1 Subspace Methods

This class of methods attempts to decompose the covariance matrix into eigen subspaces for noise and subspaces for signal. In some sense this equates to a beamforming algorithm which attempts to find an angle resulting in the strongest signal.

3.4.2 Maximum Likelihood

Foobar

[1] A singular matrix is one which is not invertible, meaning the determinant is 0

4 RF Chain

This chapter details the design and characterisation of the chain of antenna, low noise amplifier (LNA), lower pass filters and cabling. The cabling is important as each RF chain needs to have exactly[1] the same phase delay.

The LNAs which are used are the ZLF-500HLN from MiniCircuits. This part operates from 10 MHz to 500 MHz which is ideal for the application. The gain is approximately 21 dB across this band acording to the datasheet. The input current is a maximum of 110 mA.

[1] Some phase difference between the RF chains can and will be calibrated out, but the calibration routine is most robust when the RF chain phases are already closely matches

5 Calibration

There are a few areas where calibration needs to take place in order to ensure that the system performs as expected. What will be discussed here is work on calibrating the ADCs and calibrating the phase of the RF chain from the antennas to the output of the correlator. This RF chain calibration will be done in two stages:

- firstly, the path starting at the input of the LNAs will be calibrated as this can be easily done in the lab by injecting a phase coherent tone into all LNAs simultaneously.
- secondly, the entire RF beginning at the antennas will be calibrated by taking the system out into the field and transmitting tones from known positions

5.1 iADC

The iADCs suffer from a few mismatches between the cores which should be calibrated out for optimal performance. These include:

1. The offsets of each core should be set to 0. Each core can have its offset adjusted from -31.75 LSB to 31.75 LSB in steps of 0.25 LSB.
2. The gains of the cores should be made equal. The gain of each core can be adjusted from -1.5 dB to 1.5 dB in steps of 0.011 dB.
3. The sampling delay between the cores should be adjusted such that the sampling time between each core is as intended. This could be a phase difference of 0 for sampling independent signals in phase, or pi/2 for I/Q sampling or pi for interleaved sampling of a single stream.
4. There are other parameters which can also be calibrated such as the data ready delay adjustment or the gain compensation, but these are not very relevant for this work so will be ignored. Only the analogue gain, offset and sample delay will be calibrated for this work.

The iADC can be calibrated either in interleaved or independent mode. The algorithms are the same for each except for where the data is sourced from. Interleaved calibration sources all of its data from a single RF input, then splits the data up into what was read by each core and does core calibration. Independent calibration takes one stream of data samples from one of the RF inputs and another stream for the other input. Calibration is then done on this. In independent mode, care should be taken to ensure that the signal at each port is exactly the same in terms of amplitude and phase. The calibration process attempts to force these parameters to be equal.

The actual interpretation of the output of the ADC (as the ADC datasheet intends the binary number to be interpreted) is a number which oscillates between -1 and 1 depending on whether the differential voltage is slightly positive or slightly negative, even in the presence of no signal.

Table 7-8. Digital Output Coding (Nominal Setting)

Differential Analog Input	Voltage Level	Digital Output I or Q (Binary Coding)	Out-of-range Bit
> 250 mV	> Positive full-scale + 1/2 LSB	1 1 1 1 1 1 1 1	1
250 mV 248 mV	Positive full-scale + 1/2 LSB Positive full-scale - 1/2 LSB	1 1 1 1 1 1 1 1 1 1 1 1 1 1 1 0	0 0
1 mV -1 mV	Bipolar zero + 1/2 LSB Bipolar zero - 1/2 LSB	1 0 0 0 0 0 0 0 0 1 1 1 1 1 1 1	0 0
-248 mV -250 mV	Negative full-scale + 1/2 LSB Negative full-scale - 1/2 LSB	0 0 0 0 0 0 0 1 0 0 0 0 0 0 0 0	0 0
< -250 mV	< Negative full-scale - 1/2 LSB	0 0 0 0 0 0 0 0	1

Figure 5.1: ADC input differential voltage vs output binary number. Src: iADC datasheet

It does not have a concept of 0. This is shown in Figure 5.1. However, the data structures of the FPGA gateware certainly do have a concept of 0. As a result, they incorrectly interpret this number as -1 to 0. This causes the signal to have a spurious DC offset. To compensate for this, the iADC is calibrated by applying a positive offset to the output number such that it is centered around 0 and hence does not have a DC offset.

6 ROACH Firmware Design

Here are the steps which were done to produce the hardware for testing purposes. Discussion emphasis is on what I changed or modified. Blocks which were already in existance are discussed in less detail.

6.1 Software Setup

CentOS which is the open source version of RHEL. Computer with at least 8 GB of memory as the compile process is memory intensive. Number of CPU cores is not important as the Xilinx compile process only runs single threaded. Xilinx SysGen 14.7. MATLAB R2012B. Casp

6.2 ADCs

The ADCs which were available for use were the CASPER iADCs. These are 8-bit, dual core ADCs, where each core runs at 800 MHz. The cores can either be interleaved to sample a single antenna at 1600 MHz or 2 antennas at 800 MHz each.

6.3 Polyphase Filter Bank

Consists of a polyphase FIR filter which applies a window to the input signal in order to prevent spectral leakage followed by a FFT block. FFT consumes most resources and thus some optimisations had to be done to it. 4K PFB. FFT was a real FFT block meaning it only outputs the upper half spectrum as the lower half is the same due to input signals being real.

Shifting schedule set by software. Bit growth occurs at each stage. If the output of a stage is not shifted down by 1, it risks overflowing. However, if shifting is done unnecessarily, dynamic range is reduced as lower bits are thrown away. Algorithm coded to find optimal shifting. Discuss algorithm here.

6.4 Cross Multiplier

After the FFT, each antenna combination is multiplied together, one being the original signal and one being the complex conjugate. This is somewhat equivalent to dividing the complex numbers, where the key output is that the phase difference between the two antennas is produces. Some maths here to show that this is true.

Optimisations done here: these are fairly large multiplier. Each pair of antennas requires an 18 bit multiplier for the real and imag components, for both simultanious channels. This means 4 18-bit multipliers for 10 combinations. 40 x 18-bit multipliers is a lot of hardware! To mitigate this, I made a change to the complex multiplier block to allow selecting of DSP48E for multipliers. This change was committed back into the centeral code repo for all to use.

Output of a 18_17 x 18_17 is a 37_34.

6.5 Vector Accumulator

The output vector (2K complex elements) is accumulated by summing each element. This is accumulated to a 48 bit number, hence allowing for substantial growth. This is key to getting a very good phase difference approximation as uncorrelated noise is integrated out. The vector accumulator is implemented by two DSP48E blocks, one for the real and one for the imag components. This is followed by a bram which stores and feeds back the vector to the DSP48E adder.

The design is such that 48 bits are continuously accumulated. After the accumulation has run for a configurable number of iterations, the most significant 32 bits are sliced off and snapped. By accumulating 48 bits, no data is thrown away until the snap. Commit XXXXX makes this change to the dsp48_bram_vacc block in the casper library.

7 Software Interface

7.1 Code Structure

It was necessary to write code to allow the computer to interface with the correlator running on the ROACH. The code had to be carefully designed in accordance with good object orientated design methodologies in order to provide a useful, well defined and easily extendible interface to other code which needs to interface with the correlator. As such, there was significant emphasis encapsulating logic into classes which mirrored the physical structure of the correlator in the sense of modularising the key components and writing reusable code. Following is a discussion of the software interface to the correlator with specific focus on the various classes and interfaces.

Instance of a correlator is created. This then includes:

1. An instance of a ControlRegister
2. Multiple instances of Snapshot classes. One will be created for each snapshot block on the FPGA.
3. Multiple instance of the Correlation clas, one for each of the cross correlation baselines.

The direction finder code takes an instance of a correlator which can then be used for easy access to the data from the orrelator.

7.1.1 Control Register

The control register naturally lends itself to a class with interfaces to modify the different bit groups of the register in logical ways. A python module called software_register was written with a single class: ControlRegister. This class contains a value parameter which mirrors the value programmed into the FPGA's control register. It then has the following interface methods:

pulse_sync Toggles the syncronisation reset bit low to high and then high to low.

block_trigger ; allow_trigger These methods either set of clear bit the bit that controls the gate which blocks or allows the snapshot blocks being triggered by a complete accumulation. The idea is that this will be used to allow all of the snapshot blocks to be armed sequentially before they can be triggered all at once.

reset_accumulation_counter Pulses the bit which resets the counter which increments every time an accumulation completes and triggers the snap blocks. This counter lets us keep track of how many accumulations have been performed by the system.

pulse_overflow_rst Similar to the above, except this clears the latch which gets latched high whenever the FFT block overflows. This essentially allows us to 'acknowledge' that we have seen the occurrence of the overflow flag.

select_adc Controls which of the four RF inputs is connected to the time domain snapshot block via a multiplexer. By multiplexing the steams, it saves the logic and BRAM of having to have four seperate snap blocks, at the expense of one multiplexer and not being able to synchronously sample the ADC streams in the time domain. This is considered an acceptable tradeoff due to the fact that the time domain snap is only designed to be used for getting an approximation of the signal strength arriving at an antenna and this does not need to be done in parallel for each antenna.

set_shift_schedule This methods takes a 12 bit number and sets the FFT shift schedule to that number. While this design only has a 10 stage FFT, 12 bits is kept in the register for future expansions.

All of the methods in this class log their actions as well as the new value of the control register when it is modified at the debug log level.

8 Field Trials

8.1 Power supply

It was necessary to power the ROACH from a battery in order to allow it to be portable and taken out into the open field. Initially the plan was to power it from an inverter running off of a battery. Here, discuss why the inverter may be too noisy. Can this be shown from reverb chamber measurements?

Instead, an ATX power supply which runs directly from a 12 V battery was made available from the SKA equipment. The power supply is made by Mini-Box and its part number is PicoPSU-80-WI-32V. This can output 80 W which is enough to run the ROACH. To connect it, the traditional mains-powered ATX powersupply is disconnected from the motherboard and this module is plugged into the motherboard. This is shown in (insert figure here!).

Furthermore, a ROYAL 1150K battery was supplied. This is a 105 A h deep cycle calcium battery. As the ROACH draws X amps at 12 V, this implies that we are discharging the battery at $\frac{105}{X} = \frac{C}{Y}$. It is advised to not run down below 70 % to maintain the battery lifespan. As shown by (cite battery charging), this implies that the voltage should not drop to below 12.1 V when discharging at $\frac{C}{Y}$

Testing in the lab showed that the ROACH pulled 3.1 A at 12 V which is 37 W. This can easily be handled by the 80 W ATX power supply. Testing by running the ROACH from the battery overnight. The battery started at 12.6 V and had dropped to 11.9 V 15 h later. The purpose of this test was not to provide a comprehensive report of the capacity of the battery or the requirements of the ROACH, but simply to show that the system will easily be able to run for a few hours in the field during field trials.

8.2 Signal Source

The signal source used is a portable HAM radio, lent by Jason Manley of the SKA. It's rated output power is 5 W. Free space path loss equation will be calculated to get an approximation of the power going into the LNAs and the power going into the ADCs. At 2500 MHz, $\lambda = 1.2$ m. The maximum gain of the FD-250 folded dipole is approximately 0 dBi.

$$P_r = P_t G_t G_r \left(\frac{\lambda}{4\pi R}\right)^2 \tag{8.2.1}$$

$$= 5\,\mathrm{W} \times 1 \times 1 \left(\frac{1.2\,\mathrm{m}}{4\pi \times 60\,\mathrm{m}}\right)^2 \tag{8.2.2}$$

$$= 0.000\,012\,7\,\mathrm{W} \tag{8.2.3}$$

$$= 0.0127\,\mathrm{mW} \tag{8.2.4}$$

$$= -19\,\mathrm{dBm} \tag{8.2.5}$$

After the 20 dB gain of the ZFL-500HLN LNAs, the power into the iADCs is approximately

1 dBm. Seeing as the ADC's full scale range is 0 dBm, a 10 dB attenuation will be inserted after each LNA to bring the input signal down to a safe level.

9 User Interface

The UI is modeled on that presented in [16].

Bibliography

[1] R. Poisel, *Electronic warfare target location methods.* Artech House, 2012.

[2] P. Clancey. Japanese radio communications and radio intelligence. HyperWar. Accesses 2015-09-09. [Online]. Available: http://ftp.ibiblio.org/hyperwar/USN/ref/KYE/CINCPAC-5-45/index.html

[3] H. Krim and M. Viberg, "Two decades of array signal processing research: the parametric approach," *Signal Processing Magazine, IEEE*, vol. 13, no. 4, pp. 67–94, 1996.

[4] A. Sleiman and A. Manikas, "Antenna array manifold: A simplified representation," in *Acoustics, Speech, and Signal Processing, 2000. ICASSP'00. Proceedings. 2000 IEEE International Conference on*, vol. 5. IEEE, 2000, pp. 3164–3167.

[5] H. Karimi and A. Manikas, "Manifold of a planar array and its effects on the accuracy of direction-finding systems," in *Radar, Sonar and Navigation, IEE Proceedings-*, vol. 143, no. 6. IET, 1996, pp. 349–357.

[6] I. Dacos and A. Manikas, "Estimating the manifold parameters of one-dimensional arrays of sensors," *Journal of the Franklin Institute*, vol. 332, no. 3, pp. 307–332, 1995.

[7] T. E. Tuncer and B. Friedlander, *Classical and modern direction-of-arrival estimation.* Academic Press, 2009.

[8] D. Farrier, "Direction of arrival estimation by subspace methods," in *Acoustics, Speech, and Signal Processing, 1990. ICASSP-90., 1990 International Conference on.* IEEE, 1990, pp. 2651–2654.

[9] E. C. Desk, "Electronic warfare and radar systems engineering handbook," 1997.

[10] H. H. Jenkins, *Small-aperture radio direction-finding.* Artech House, 1991.

[11] R. Grabau and K. Pfaff, "Funkpeiltechnik," *Stuttgart: Franckh'sche Verlagshandlung, W. Keller & Co*, pp. 350–351, 1989.

[12] P. J. Gething, *Radio direction finding and superresolution.* IET, 1991, no. 33.

[13] R. A. Poisel, *Introduction to communication electronic warfare systems.* Artech House, Inc., 2008.

[14] I. Pellejero. Adcock/watson-watt radio direction finding. Accessed 2015-09-01. [Online]. Available: http://www.ipellejero.es/tecnico/adcock/english.php

[15] Radiomonitoring and R. Catalog, "Introduction into theory of direction finding," Rhode & Schwarz, Tech. Rep., 2011/2012. [Online]. Available: http://rohde-schwarz-ad.com/docs/ewtest/intro_theory_of_direction_finding.pdf

[16] D. Guerin, "Passive direction finding," Ph.D. dissertation, MIT Lincoln Laboratory, 2012.